Soil Dynamics and Earthquake Engineering 78 (2015) 61–70

Contents lists available at ScienceDirect

Soil Dynamics and Earthquake Engineering

journal homepage: www.elsevier.com/locate/soildyn

Quasi-3D analysis: Validation by full 3D analysis and field tests on single piles and pile groups

Guoxi Wu [a], W.D. Liam Finn [b], Jason Dowling [b,*]

[a] BC Hydro, 6911 Southpoint Drive, Burnaby, BC, Canada, V3N 4X8
[b] The University of British Columbia, 2002-6250 Applied Science Lane, Vancouver, BC, Canada, V6T 1Z4

ARTICLE INFO

Article history:
Received 17 September 2014
Received in revised form
7 July 2015
Accepted 8 July 2015

Keywords:
Piles
Pile group
Lateral load
Quasi-3D
Finite element
Transmitting boundaries

ABSTRACT

A quasi-3D method for the analysis of single piles and pile groups is presented. The method includes an equivalent linear constitutive model for nonlinear analysis, an 8-node pile element that simulates the effects of pile volume and energy transmitting boundaries which are especially important for the analysis of high frequency loading of machine foundations. The quasi-3D formulation and equivalent linear model result in orders of magnitude decreases in computational time. The accuracy and reliability of the approximate approach was validated by comparing results with 3D analytical results from MIT and by data from field tests on single piles and pile groups from Taiwan. The computed results compared very favorably with the analytical and field test data.

1. Introduction

Full-scale lateral load tests on bored and driven precast piles, both single piles and pile groups, were carried out in Chaiyi, Taiwan by Huang et al. [1]. They conducted numerical analyses of the laterally loaded single piles using *p*–*y* curves to model soil–pile interaction [2,3]. The *p*–*y* curves were derived from in-situ DMT (dilatometer tests). The laterally loaded pile groups were analyzed using the concept of *p*-multipliers [4,5] to account for pile–soil–pile interaction in the group. The *p*-multipliers for both the bored and driven pile groups were back-calculated from the Chaiyi lateral group load tests reported by Huang et al. [1]. The *p*-multipliers were $p=0.70$ for driven piles and $p=0.79$ for bored piles.

Mostafa and El Naggar [6] computed dynamic *p*-multipliers of the two pile groups using a combination of static *p*–*y* curves and a plane strain assumption [7] to represent the soil reaction within the framework of a Winkler model. They obtained good comparisons with Huang et al. [1], when they used *p*-multipliers of $p=0.94$ for driven piles and $p=0.75$ for bored piles. These results show that the *p*-multipliers are dependent on the computational model and this introduces major uncertainty in any analysis in the absence of site specific load tests to calibrate the *p*-multipliers. Another cause of problems with the *p*-multiplier is the inherent unreliability of the *p*–*y* curves that underpin the *p*-multiplier approach. O'Neill and Gazioglu [8] and Murchison and O'Neill [9] made a detailed study of the capability of the *p*–*y* curves recommended by the American Petroleum Institute [10] to predict the performance of full scale load tests on single piles. They found the reliability of pile performance predictions using these *p*–*y* curves to be low. In an attempt to overcome these problems, a continuum finite element model, PILE-3D, was developed by Wu [11] and Wu and Finn [12,13] to analyze the response of single piles and pile groups subject to dynamic lateral loads, using an equivalent linear constitutive model. Since then, the method has been applied both in research and in practice, [14,15,16,17,18].

An improved version of PILE-3D, called VERSAT- P3D, was introduced by Wu [19] and has been used in other studies by Finn and Wu [20] and Finn and Dowling [21]. The new version has energy transmitting boundaries and an enhanced pile model that simulates the effect of pile volume on pile–soil interaction. PILE-3D simulated the pile by a beam element only, with no account of pile volume.

Prior to the analysis of the lateral load tests of Huang et al. [1], VERSAT-P3D is first extensively validated by comparing its solutions with the full 3D solutions of Kaynia and Kausel [22] for both single piles and pile groups. VERSAT-P3D is then used to analyze the lateral response of the bored and driven single piles and pile groups tested by Huang et al. [1]. The nonlinear analyses were

* Corresponding author.
E-mail addresses: gwu@wutecgeo.com (G. Wu), finn@civil.ubc.ca (W.D. Liam Finn), jadowlin@mail.ubc.ca (J. Dowling).

http://dx.doi.org/10.1016/j.soildyn.2015.07.006
0267-7261/

List of symbols

G^*	complex shear modulus of soil
G_E	shear modulus of the sub-stratum
L	pile length
d	pile diameter
E_p	Young's modulus of pile
E_s	Young's modulus of soil
v	displacement in the y direction
λ	hysteretic damping ratio of soil
ρ_s	mass density of soil
ρ_E	the mass density of sub-stratum
μ	Poisson's ratio of soil
θ	parameter related to the Poisson ratio as, $\theta=2/(1-\mu)$
V_s	shear wave velocity of soil
v_S	shear wave velocity of the elastic sub-stratum
τ_B	shear stress being transmitted across the boundary between the soil deposit and the underlying medium
x_e	horizontal displacement of a material particle located at depth z_e
x_I	displacement component due to the incident wave
V_I	velocity component due to the incident wave
x_R	displacement component due to the reflected wave
V_R	velocity component due to the reflected wave
V_B	the particle velocity at the boundary
V_{IB}	the particle velocity component at the boundary due to the incident wave
V_{RB}	the particle velocity component at the boundary due to the reflected wave
ω	dynamic load frequency
k_{yy}	horizontal stiffness
$k_{\theta\theta}$	rotational stiffness
k_{zz}	vertical stiffness
k_{zz}^0	static vertical stiffness of single piles
a_0	dimensionless frequency, $a_0=\omega d/V_s$
λ_{a0}	damping constants, defined as in Eq. (7)
K	complex stiffness
k	static stiffness
c	damping constant (defined in formulation of dynamic impedance $K=k+ia_0c$)
k^0	stiffness of an identical single pile, to those in a group of interest, placed in the same soil medium
s/d	space-to-diameter ratio of piles within a group
α_{yy}	group factor for horizontal stiffness
α_{zz}	group factor for vertical stiffness
$\alpha_{\varphi\varphi}$	group factor for rocking stiffness
$k_{\varphi\varphi}^g$	rocking stiffness of a fixed-head pile group
$k_{\varphi\varphi}^{cap}$	rocking stiffness of the pile cap
$k_{\theta\theta}$	rotational stiffness at the head of a pile in a group
r_i	distance of a pile to the centerline of rocking
F_i	axial force at a pile head subjected to a unit rotation of the pile cap
E_d	average dilatometer moduli determined from the DMTs
EI	flexural rigidity

carried out using the strain-dependent soil moduli and damping ratios of the equivalent linear constitutive model and taking into account yielding at failure and a no-tension cut-off. The response of the pile groups is computed directly without having to use either p–y curves or p-multipliers. A description of the enhanced model is described in the next section.

2. Verification: quasi-3D vs 3D

2.1. The VERSAT-P3D finite element model

Under vertically propagating shear waves (Fig. 1) the foundation soils undergo mainly shearing deformations in the xoy plane, except in the area near the pile where extensive compression deformations develop in the direction of shaking. The compressive deformations also generate shearing deformations in the yoz plane as shown in Fig. 1.

The quasi-3D method proposed by Wu [11] and Wu and Finn [12,13] simplified the model formulation by assuming that dynamic motions are governed primarily by shear waves in the xoy and yoz planes and compression waves in the direction of shaking, y. Based on these assumptions, they developed Eq. (1) for describing the free vibration of the soil continuum

$$\rho_s\frac{\partial^2 v}{\partial t^2} = G^*\frac{\partial^2 v}{\partial x^2} + \theta G^*\frac{\partial^2 v}{\partial y^2} + G^*\frac{\partial^2 v}{\partial z^2} \tag{1}$$

where v is displacement in the y-direction, and G^* is a complex shear modulus. The complex shear modulus G^* is expressed as $G^*=G\ (1+i2\lambda)$. The parameter θ was shown to be $\theta=2/(1-\mu)$, where μ is the Poisson ratio, assuming a plane strain condition in the y direction [23].

This computational model is enhanced in VERSAT-P3D [19] by implementing an 8-node pile element to account for the effect of

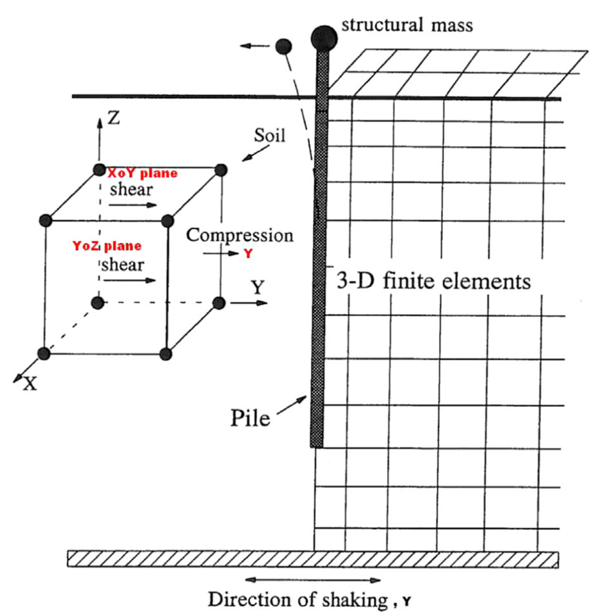

Fig. 1. VERSAT-P3D finite element model in horizontal y-direction (after Wu [11]).

pile diameter and the incorporation of energy transmitting boundaries. These boundaries are especially important for the analysis of high frequency vibrations such as machine foundation response. The 8-node pile element is a bending structural element that consists of four beam elements arranged at the four sides of an 8-node brick element that has the same volume as the pile and the same bending stiffness. At any level the displacements of the nodes of the pile element are constrained to have the same displacement. Both translation and rotation are permitted at each pile node to capture the bending behavior of the pile. The soil is modeled using an 8-node brick element also. The soil element uses the equivalent linear constitutive model comprising the strain-dependent soil moduli and damping ratios of the, yielding at failure and a no-tension cut-off described above. Development of gaps between the pile and soil is not permitted.

The rocking of the pile foundation involves vertical displacements and must be calculated separately. A fully coupled analysis would necessitate a full 3-D formulation thus losing much of the computational advantage of the quasi-3-D approach. The computational pattern is a follows. At time t the rocking is computed using the current soil properties in the foundation. A time $t+\Delta t$ the analysis is returned to the horizontal mode with updated soil properties. This alternating process is continued to the end of the excitation.

2.2. Energy transmitting boundary conditions

The finite models of pile foundations are separated from the infinite half-space below by an energy transmitting boundary that allows waves in the model to leak into the half-space below. The loss of the energy carried by these waves is simulated by incorporating a viscous dashpot in the model. The properties of the dashpot are formulated below.

The viscous dashpot model formulated by Joyner and Chen [24], is incorporated into VERSAT-P3D.

The method evaluates the shear stress, τ_B, being transmitted across the boundary between the soil deposit and the underlying medium. This underlying medium is assumed to be elastic and the propagating shear waves are plane waves traveling vertically. If x_e is the horizontal displacement of a material particle located at depth z_e, on the boundary, then

$$\tau = G_E\left(\frac{\partial x_e}{\partial z_e}\right) \tag{2}$$

where G_E is the shear modulus of the sub-stratum. If x_I, V_I and x_R, V_R are the displacement and velocity components due to the incident and reflected waves, respectively, then,

$$x_I = x_I(z_e + \nu_S t) \tag{3a}$$

$$x_R = x_R(z_e - \nu_S t) \tag{3b}$$

where ν_S is the shear wave velocity of the elastic sub-stratum. Eqs. (2) and (3a) and (3b) give,

$$\tau = G_E\left(\frac{\partial x_I}{\partial z_e} + \frac{\partial x_R}{\partial z_e}\right) = G_E\left(\frac{V_I}{\nu_S} + \frac{V_R}{\nu_s}\right) \tag{4}$$

The shear stress at the boundary becomes

$$\tau_B = G_E \frac{(V_{IB} - V_{RB})}{\nu_S}\Bigg|_{z_e = z_B} \tag{5}$$

Note that $V_B = V_{IB} + V_{RB}$, where V_B is the particle velocity at the boundary, V_{IB} is the particle velocity component at the boundary due to the incident wave, V_{RB} is the particle velocity component at the boundary due to the reflected wave, and $G_E = \rho_E \nu_S^2$, ρ_E is the density of sub-stratum. Finally, the resulting equation for the shear stress at the boundary becomes

$$\tau_B = \rho_E \nu_s (2V_{IB} - V_B) \tag{6}$$

2.3. Verification of VERSAT-P3D

VERSAT-P3D models the more important aspects of pile response to horizontal loads but not the full 3D response. Therefore it is necessary to assess the potential accuracy of the program against full 3D analysis. Full 3D analytical solutions are only available for elastic media. The rigorous elastic solutions by Kaynia and Kausel [22] are used for verification.

The dynamic stiffnesses at the pile head for single piles in an elastic soil medium were computed as a function of dynamic load frequency, ω, using VERSAT-P3D. The analyses were conducted for piles with two diameters (0.3 m and 0.76 m) and a pile–soil system with E_p/E_s of 1000, L/d of 15, where L and d are pile length and diameter respectively, μ of 0.4 and λ of 5%. The computed horizontal stiffness (normalized to $k_{yy}/E_s d$), rotational stiffness (normalized to $k_{\theta\theta}/E_s d^3$) and vertical stiffness (normalized to $k_{zz}/E_s d$) are plotted against the dimensionless frequency $a_0(=\omega d/V_s)$ and compared with those reported by Kaynia and Kausel [22] in Figs. 2–4. These figures also show the equivalent values reported in Kaynia and Kausel [22] for comparison. Wu and Finn [12] also reported these values for comparison, but were only capable of achieving acceptable results up to a dimensionless frequency $a_0 = 0.3$. The new approach gives accurate results up to $a_0 = 1.0$.

Fig. 5 shows the horizontal and vertical damping constants, λ_{a0}, defined as in Eq. (7).

$$\lambda_{a0} = \frac{c}{Nk^0} \tag{7}$$

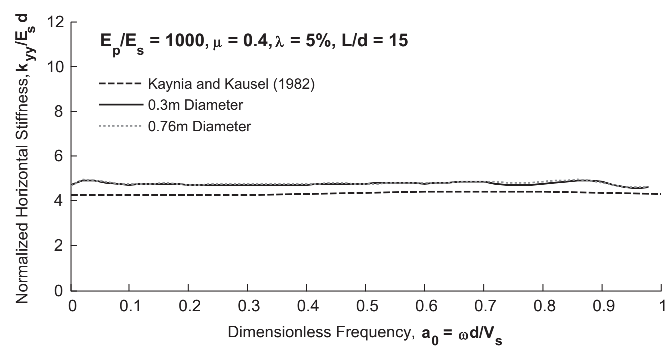

Fig. 2. Normalized horizontal stiffness of single piles.

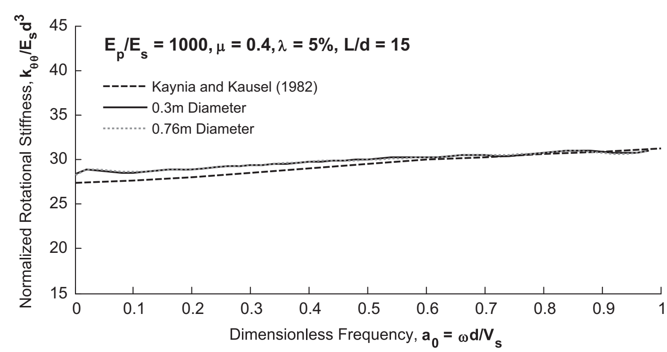

Fig. 3. Normalized rotational stiffness of single piles.

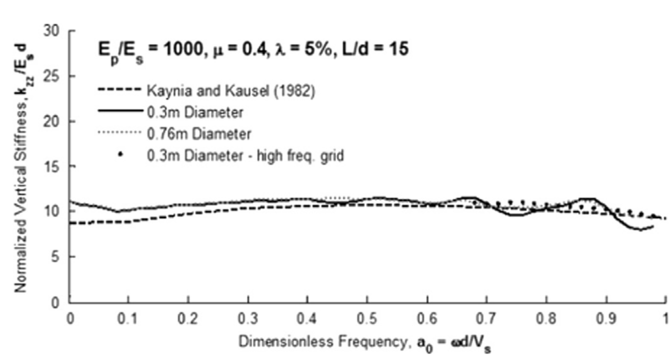

Fig. 4. Normalized vertical stiffness of single piles.

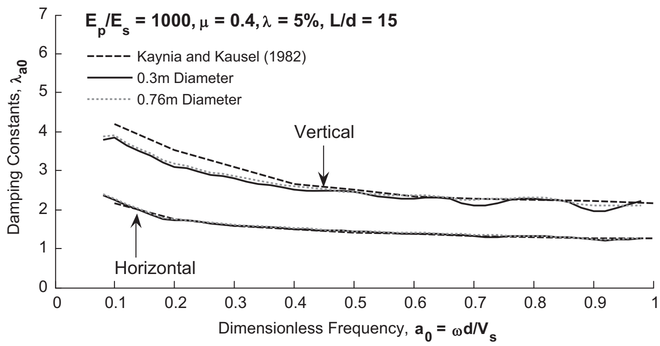

Fig. 5. Horizontal and vertical damping constants (λ_{a0}) for single piles.

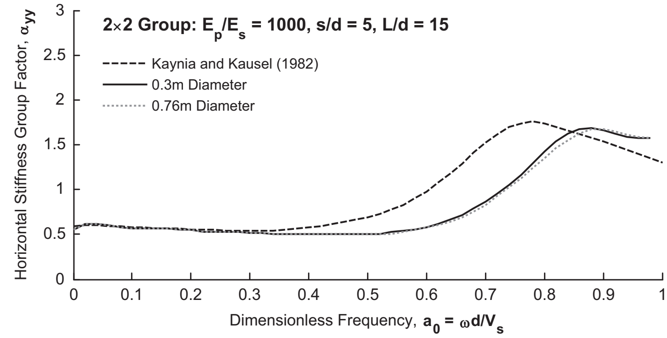

Fig. 6. Group factors for horizontal stiffness of 2×2 pile groups.

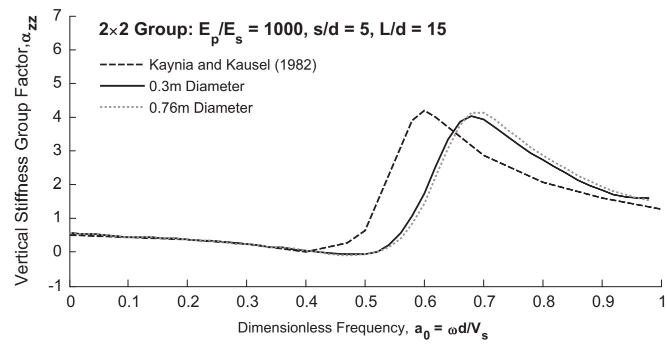

Fig. 7. Group factors for vertical stiffness of 2×2 pile groups.

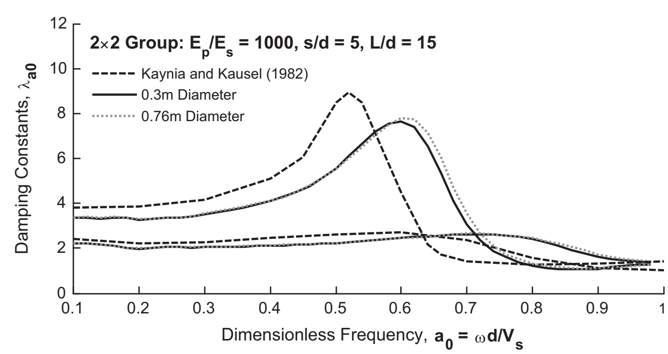

Fig. 8. Horizontal and vertical damping constants (λ_{a0}) for 2×2 pile groups.

where c is defined in formulation of dynamic impedance $K=k+ia_0c$, where K is the complex stiffness and k is the static stiffness [27]; N is the number of piles in a pile group ($N=1$ for single piles); and k^0 is the static stiffness of an identical single piles placed in the same soil medium.

The grid size for all single piles simulations is $12\times36\times29$. That is, 12 elements in the x (out-of-plane) direction, 36 elements in the y direction, or direction of shaking, and 29 elements in z (vertical) direction. Grid spacing increases with the distance of grid line from the piles and is the largest at the model boundaries. The model dimensions ($x\times y\times z$) are 8.32 m × 26 m × 12 m for the 0.3 m diameter pile simulation and 19.72 m × 67.32 m × 32 m in the case of the 0.76 m diameter pile. The results from VERSAT- P3D are in good agreement with the rigorous solutions from Kaynia and Kausel [22] in all cases, with the exception of the vertical stiffness shown in Fig. 4. In this case some small oscillations occur at dimensionless frequencies $a_0>0.7$, or a vibration frequency of 210 rad/s for a site with $V_s=90$ m/s and a pile diameter of 0.3 m. To improve the accuracy at dimensionless frequencies $a_0>0.7$, a finer mesh is required than the standard mesh. The dotted points show the response from the finer mesh, and it is clear that it fits the results from Kaynia and Kausel [22] very well.

Therefore, as a general rule of thumb, the standard grid, $12\times36\times29$, is good for a nonlinear analysis with relatively low frequency, such as for seismic loading conditions, where the application requires a far-field (or free field) zone to differentiate it from the influence of the piles. But the standard grid may not be satisfactory for analysis of high-frequency vibrations as the large grid size can often truncate the high frequency response.

Verification analyses were also conducted for 2×2 pile groups with a space-to-diameter ratio of $s/d=5$. The piles are assumed to be rigidly fixed to the pile cap. All other parameters are the same as those for analyses of single piles. The group factors for horizontal stiffness (α_{yy}) and vertical stiffness (α_{zz}) are defined as in Eqs. (8) and (9)

$$\alpha_{yy}=\frac{k_{yy}}{Nk_{yy}{}^{0}} \tag{8}$$

$$\alpha_{zz}=\frac{k_{zz}}{Nk_{zz}{}^{0}} \tag{9}$$

where k is defined in $K=k+ia_0c$; and k^0 is the static stiffness of a single piles (Note: subscripts yy and zz denote horizontal and vertical components, respectively). The group factors, α_{yy} and α_{zz}, are plotted against a_0 and compared with those reported by Kaynia and Kausel [22] in Figs. 6 and 7, respectively. The horizontal and vertical group damping constants, λ_{a0} (defined in Eq. (7)), are presented in Fig. 8.

Once again, the results for the 2×2 pile groups from the quasi-3D method are in good agreement with the rigorous solutions of Kaynia and Kausel [22] up to a dimensionless frequencies $a_0<0.5$, but beyond this a finer mesh would be required as discussed in relation to Fig. 4. The maximum horizontal and vertical stiffness from this study occurs at higher a_0 values of approximately 0.9 and 0.67, respectively, instead of 0.8 and 0.62 as obtained by Kaynia and Kausel [22]. The difference in frequency at which the maximum stiffness occurs is in general within 10%. The model of the 2×2 pile group used the standard built in $12\times36\times29$ element grid. The model dimensions ($x\times y\times z$) are 8.29 m × 25.94 m × 12 m for the 0.3 m diameter pile group and 19.58 m × 67.04 m × 32 m in the case of the 0.76 m diameter pile group. As mentioned above, these results can be improved by using a finer mesh.

For a fixed-head pile group, the rocking stiffness of the pile group ($k^{g}_{\varphi\varphi}$) consists of both rocking stiffness of the pile cap ($k^{cap}_{\varphi\varphi}$) and the sum of the rotational stiffness, $k_{\theta\theta}$, at the head of each pile in the group. The group factors for rocking stiffness ($\alpha_{\varphi\varphi}$) are defined as in Eq. (10)

$$\alpha_{\varphi\varphi}=\frac{k_{\varphi\varphi}{}^{g}}{k_{zz}{}^{0}\bullet\sum r_i{}^2} \tag{10}$$

where $k^{g}_{\varphi\varphi} = k^{cap}_{\varphi\varphi} + \sum k_{\theta\theta}$ and $k^{cap}_{\varphi\varphi} = \mathrm{Re}\{\sum r_i \bullet F_i\}$; r_i is the distance of a pile to the centerline of rocking; F_i is the axial force at a pile head subjected to a unit rotation of the pile cap [12] assuming all piles are pinned to the pile cap; and k^{0}_{zz} is the static vertical stiffness of a single piles.

3. Field tests of Huang et al. [1]

Huang et al. [1] tested the Bored Pile (BP) group of 6 piles and the driven Precast Concrete (PC) pile group of 12 piles shown in Fig. 9. Piles in each group were cast into a solid pile cap as detailed in Huang et al. [1]. A jack and load cell system was installed between the two pile groups to apply the lateral forces for lateral load tests on the two pile groups. Lateral load tests on single piles were conducted on piles B7, B13 and P7. All piles were spaced at a center-to-center distance of 3 times the diameter of piles in each group. The PC piles are hollow but infilled with concrete. The structural properties of both the bored piles and the PC piles are listed in Table 1.

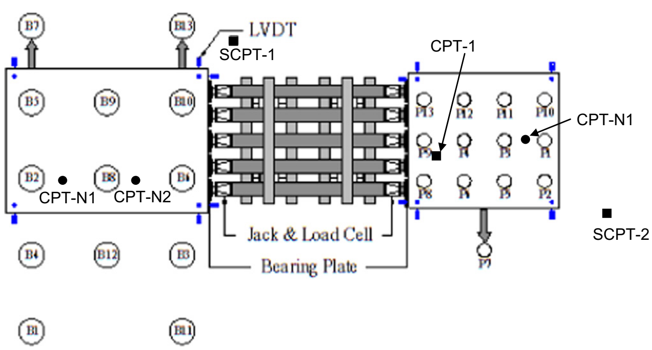

Fig. 9. Layout of test piles and CPT test holes, after Huang et al. [1].

Table 1
Structural properties of piles (Huang et al. [1]).

Item	Bored piles	PC piles
Diameter	1.5 m	0.8 m OD, 0.56 m ID with concrete infill
Length (m)	34.9	34
Intact flexural rigidity. *EI* (kN m^2)	6.86×10^6	0.79×10^6

Table 2
Soil profile and parameters used in VERSAT-P3D analyses.

Soil layer no.	Depth [a] (m)	Soil type	Soil density (kN/m^3)	Shear modulus (MPa)	Poisson's ratio (μ)	Tension strength (kPa)	Yield strength (kPa)
M3	1	Sandy silt	18	5.7	0.4	11	10
M4	2	Sandy silt	18	5.7	0.4	15	14
M5	3	Sandy silt	18	5.7	0.4	19	18
M6	4.2	Silty sand	19.5	33.3	0.35	48	34
M7	5.4	Silty sand	19.5	33.3	0.35	65	45
M8	6.5	Silty sand	19.5	33.3	0.35	65	45
M9	8	Silt	18	10.3	0.45	VH[b]	VH[b]
M10	9.5	Silt	18	10.3	0.45	VH[b]	VH[b]
M11	11	Silt	18	10.3	0.45	VH[b]	VH[b]
M12	12.5	Silty sand	19.5	48	0.35	VH[b]	VH[b]
M13	14.5	Silty sand	19.5	48	0.35	VH[b]	VH[b]
M14	18	Silt and sand	19	48	0.4	VH[b]	VH[b]
M14	22	Silt and Sand	19	48	0.4	VH[b]	VH[b]
M15	26	Silt	18.5	11	0.45	VH[b]	VH[b]
M15	30	Silt	18.5	11	0.45	VH[b]	VH[b]
M16	33	Silty sand	20	48	0.35	VH[b]	VH[b]
M16	39	Silty sand	20	48	0.35	VH[b]	VH[b]

[a] Depth is from the underside of the pile cap.
[b] Very high (VH) values are assigned to the soil layers when they are considered to be non-yield or non-tension materials.

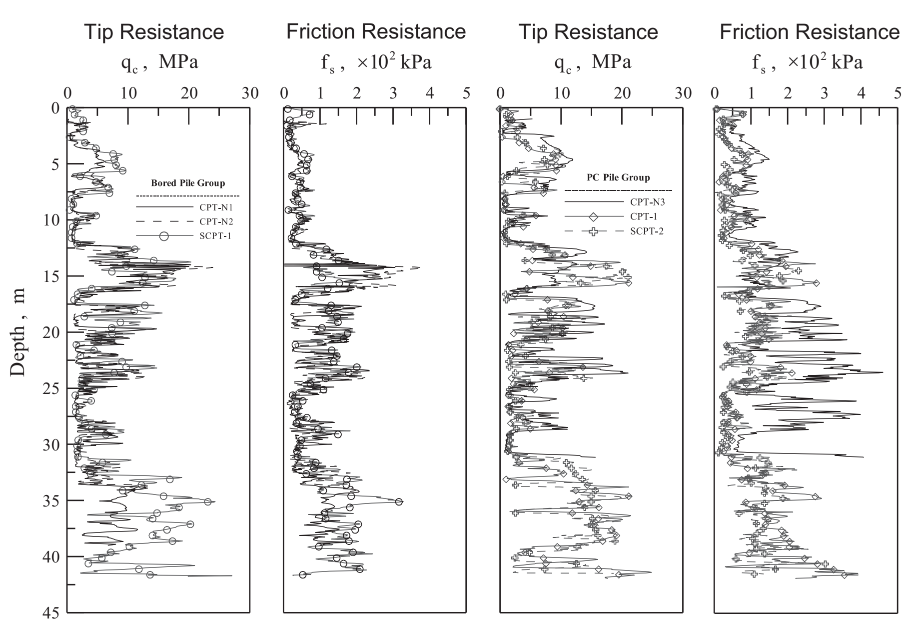

Fig. 10. Cone Penetration Test (CPT) data from the site, after Huang et al. [1].

Soil investigation before and after the pile installations consisted of eight boreholes to a maximum depth of 80 m, four Cone Penetration Tests (CPTs), two Seismic CPTs (SCPTs), and five dilatometer tests (DMTs). Approximate locations of the CPT holes are shown in Fig. 9 and results of the CPT tests are shown in Fig. 10. The groundwater table was located at approximately 1 m below the ground surface. According to soil samples recovered from the boreholes, the soils within the 80 m depth were generally classified as silty sand to silt with occasional layers of silty clay. Average dilatometer moduli, E_d, determined from the DMTs were approximately 5.9, 30, 9.5, 48, 41.5, 13 and 50 MPa at depths of 4, 7.5, 12, 15.5, 23, 30 and 39 m, respectively.

Table 3
Flexural rigidity of single piles used in the analysis.

Load level (kN)	*EI* of P7 (kN m^2)		Load level (kN)	*EI* of B7 (kN m^2)	
	Depth 4 to 6 m	Other depth		Depth 6 to 9 m	Other depth
265	0.79×10^6	0.79×10^6	814	6.86×10^6	6.86×10^6
570	0.14×10^6	0.79×10^6	1462	1.37×10^6	6.86×10^6
736	0.10×10^6	0.79×10^6	1908	1.37×10^6	6.86×10^6
			2943	1.37×10^6	6.86×10^6

4. Analysis of the field tests

4.1. Soil parameters

The soil profile and parameters, derived from the boreholes, CPT and DMT data of the site and shown in Table 2 were used for all analyses presented in this paper. The shear moduli of each respective soil layer in Table 2 are compatible with the dilatometer moduli (E_d) measured by Huang et al. [1]. In addition, strain dependent moduli and damping factors from Seed et al. [25] for sandy soils and from Vucetic and Dobry [26] for silty soils were used for the analyses of the responses of single piles and pile groups subjected to large magnitude loads in the tests [1]. The soil properties were modified to include the effects of the water table where necessary.

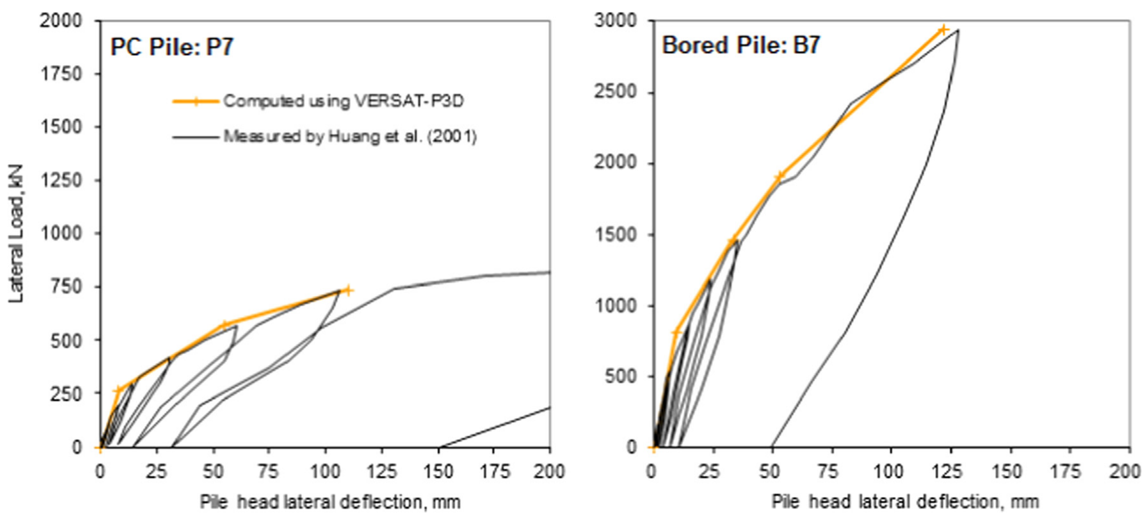

Fig. 11. Comparison of lateral load versus pile head deflections for single piles.

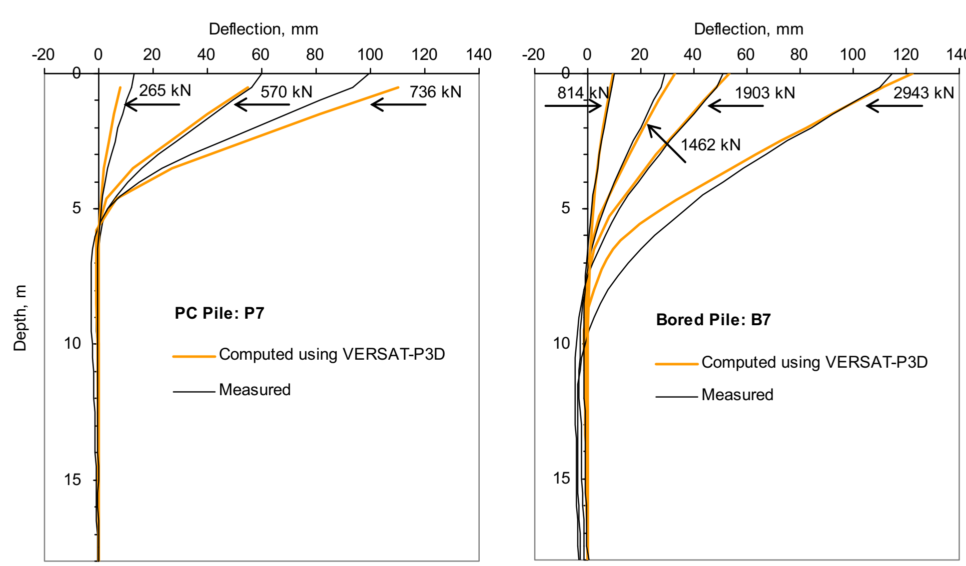

Fig. 12. Pile deflections versus depth for single piles under various load levels.

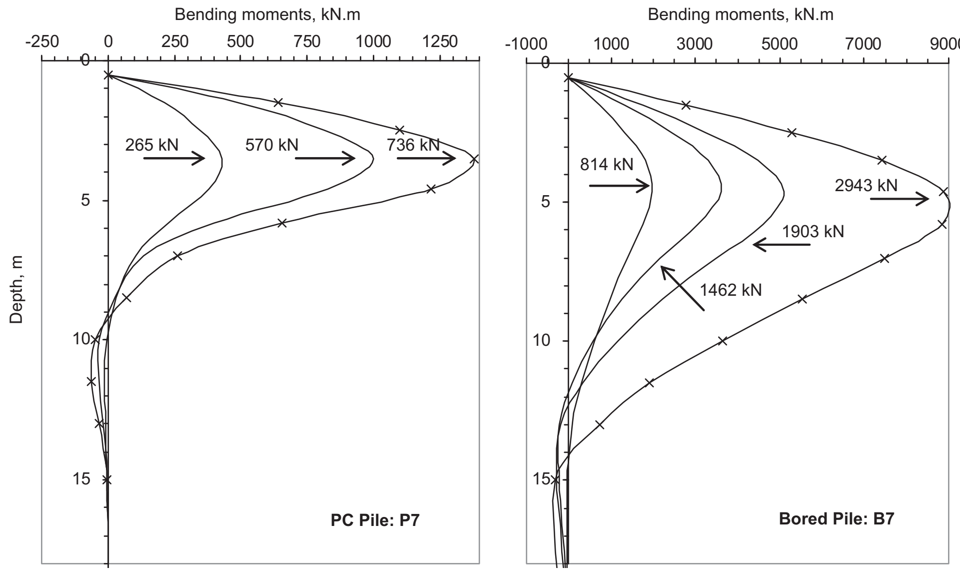

Fig. 13. Computed bending moments of piles versus depth for single piles at various load levels.

Table 4
Flexural rigidity of piles and assumed $\eta_{\phi\phi}$ for rocking stiffness of pile cap.

Load level (kN)	PC pile group		Load level (kN)	Bored pile group	
	$\eta_{\phi\phi}$	*EI* for piles		$\eta_{\phi\phi}$	*EI* for piles
2774	0.025	0.79×10^6	3284	1.00	6.86×10^6
5550	0.025	0.79×10^6	6568	1.00	6.86×10^6
7122	0.025	0.79×10^6	8348	1.00	6.86×10^6
Unit for *EI*: kN m^2			10,948	0.35	6.86×10^6

Note: Rocking stiffness of a pile group = rotational stiffness of piles + $\eta^*_{\phi\phi}$ rocking stiffness of pile cap.

4.2. Analyses for single PC and bored piles

Huang et al. [1] noted during their report of the tests that the field inclinometer measurements showed a sharp change in curvature in the measurements of pile P7, at a lateral load of 570 kN and in measurements of pile B7, at a lateral load of 1462 kN, most likely indicating that the piles cracked at these loads. A reduced flexural rigidity (*EI*) was assigned to the relevant section of these piles in order simulate section cracking (Table 3). The reduced values of *EI* were used for pile P7 for the VERSAT-P3D analyses in this study are the same as those reported by Huang et al. [1] for their analyses using the program GROUP, version 4.0 [28]. In the case of bored pile B7, the *EI* used in the VERSAT-P3D analyses is reduced to 1.37×10^6 kN m^2, in order to obtain a suitable match between the analyses and test measurements. Huang et al. [1] used 4.29 to 5.75×10^6 kN m^2. An $8\times24\times17$ grid was used for the analysis of single piles. The model dimensions ($x\times y\times z$) are 42.9 m × 134 m × 39 m for the bored pile (B7) and 22.4 m × 70 m × 39 m in the case of the PC pile (P7).

The results of the single piles analyses are shown in Fig. 11 for pile head deflection versus load level, and in Fig. 12 for pile deflection profile versus depth. The computed results are in good agreement with the measured pile deflections from the tests. The computed bending moments along the pile with depth are shown in Fig. 13 for both P7 and B7. The computed maximum bending moment is about 1000 kN m for P7 at a load level of 570 kN, and 3600 kN m for B7 at a load level of 1462 kN. The maximum bending moment has significantly exceeded the bending moment capacity of each pile indicating yielding and the occurrence of

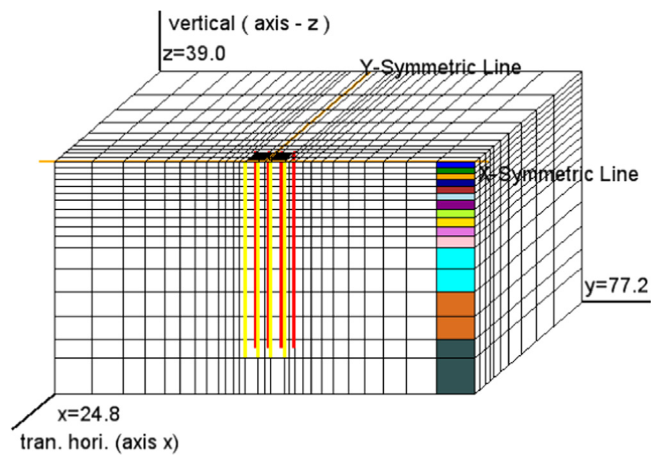

Fig. 14. Finite element mesh used for analyses of the 3×4 PC pile group.

cracks as indicated by the inclinometer tests. In a case where inclinometer tests may not have been available, one could have roughly predicted the initiation of cracking from the moments relative to max moment capacity.

The analysis to obtain the driven pile results used a coarse finite element mesh representing a physical size of 22.4 m × 70 m × 39 m, that requires about 20 min of CPU time to compute the displacement for one load point on the loading curve, on a laptop with an Intel Core i7 CPU processor (2.2 GHz). Analyses of similar problems by FLAC-3D and using a similar grid size took about 6 h [29].

4.3. Analyses of the pile groups

As noted in Huang et al. [1], there was no apparent sign of pile breakage during the load tests on the pile groups (thus 100% *EI*), but the pile-cap connection was not always rigid throughout the tests due to a moment induced at the pile head that exceeded the moment capacity of the pile or construction details or both. Inclinometer readings showed relatively large rotation at the driven PC pile-cap connection from the beginning of the test, and at the bored pile-cap connection at a load level of 9643 kN. In these cases only a portion of the rocking stiffness of the pile cap ($k^{cap}_{\varphi\varphi}$) defined as $\eta_{\phi\phi}$, is transferred to the piles. These values of $\eta_{\phi\phi}$

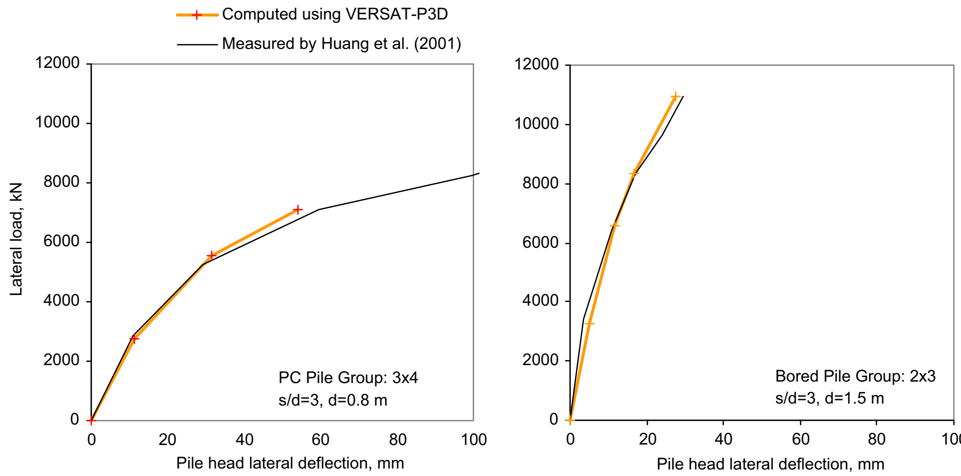

Fig. 15. Comparison of lateral load versus pile head deflections for pile groups.

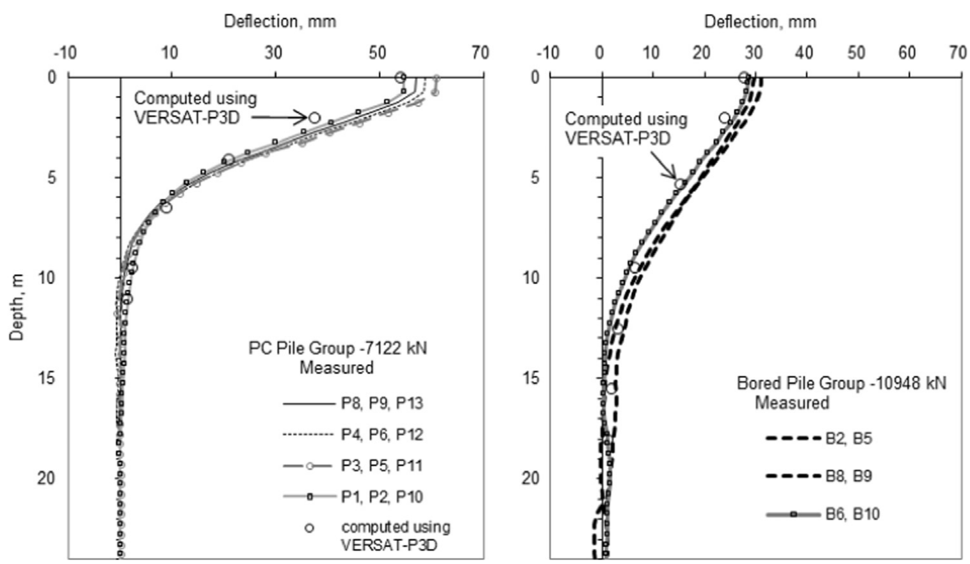

Fig. 16. Pile deflections versus depth for pile groups at a selected load level.

are given in Table 4, for the analysis of the pile group response. This value of $\eta_{\phi\phi}$ was selected to give the best fit to the measured response. As described below, though a different value of $\eta_{\phi\phi}$ may have been optimal for each different load level, an average value was used for each group. The parameter$\eta_{\phi\phi}$, is a measure of the degree of fixity of the piles to the pile cap, ranging from full fixity to the pinned condition when $\eta_{\phi\phi}$ is equal to zero.

It is noted that for the case of an analysis of a pile group that has all piles pinned to the cap, $\eta_{\phi\phi}$ is excluded from the calculated rocking stiffness. A $10 \times 26 \times 17$ grid was used for the analysis of the pile groups. The model dimensions $(x \times y \times z)$ are 45.2 m × 143.9 m × 39 m for the six-pile (2 × 3) bored pile group and 24.8 m × 77.2 m × 39 m in the case of the twelve-pile (3 × 4) PC pile group. The pile cap measured approximately 8 m × 12 m for the bored pile group and 6 m × 8.4 m for the PC pile group. Fig. 14 is presented to provide a visual example of the model used in the VERSAT-P3D analysis of the 3 × 4 PC pile group. The different colors in the vertical layers of soil elements in Fig. 14 correspond to layers with different soil properties.

The results of pile group analyses are shown in Figs. 15 and 16. In general they are in good agreement with the measured pile deflections from the tests. It is noted that the computed pile head deflections of the PC pile group are slightly higher at 2774 kN and 5550 kN, but slightly lower at 7122 kN, than the measured values. The assumed value of $\eta_{\phi\phi}$ is considered to be an average of the three. The test results may be better matched by using a slightly higher $\eta_{\phi\phi}$ at 2774 kN, but lower $\eta_{\phi\phi}$ at 7122 kN. An average value of $\eta_{\phi\phi}$ was purposely selected to show that the results of analysis are not very sensitive to$\eta_{\phi\phi}$. The computed bending moments along piles are shown in Fig. 17 for both the PC pile group and the bored pile group. It is evident that the piles located in the middle rows of a group take less bending moments than the lead/trail rows of piles, and the pile located in the center of the middle rows takes the least bending moments.

4.4. Limitations of VERSAT-P3D

VERSAT-P3D is a quasi-3D analysis program but comparisons with full 3-D analyses and data from field tests show that it achieves a high level of accuracy under both static and dynamic loading conditions. However all the dynamic input motions used with the program are assumed to be shear waves propagating vertically as is common in engineering practice. It should not be used for motions propagating at an angle to the horizontal. The program uses the equivalent linear constitutive model. This model is considered good for shear strains up to 1%.

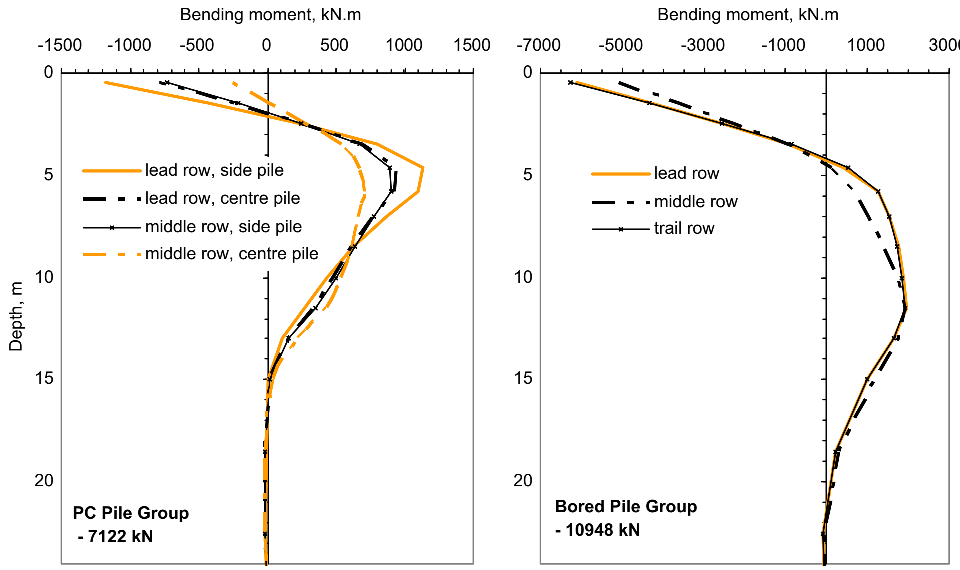

Fig. 17. Computed bending moments of piles versus depth for pile groups at a selected load level.

5. Summary

The VERSAT-P3D was developed for finite element program for response analysis of single piles or pile groups. By not using a complete 3D formulation, the computational time has been reduced by several orders of magnitude, compared with corresponding times in full 3D programs. Extensive validation has shown that the program gives very reliable results when the input motions are presented by shear waves propagating vertically.

Validation results are presented in the paper for full 3D elastic analysis under dynamic loading and for static load tests in the field for driven and bored single piles ad pile groups.

The constitutive model used in VERSAT-P3D is the widely used equivalent linear model with the addition of a yield criterion and a no-tension cut off. The accuracy of this model is acceptable for shear strains up to about 1%, but in practice it is traditionally used beyond this level.

Acknowledgments

The authors wish to thank Professor Huang of National Chiao Tung University (Taiwan) for his kind support by making the original data available.

The very helpful and insightful comments of the reviewers are gratefully acknowledged. These comments have done much to improve the context and content of the paper. This help is much appreciated.

References

[1] Huang AB, Hsueh CK, O'Neill MW, Chern S, Chen C. Effects of construction on laterally loaded pile groups. ASCE J Geotech Geoenviron Eng 2001;127(5):385–97.
[2] Matlock H. Correlations for design of laterally loaded piles in soft clay. In: Proceedings of the 2nd offshore technical conference. Dallas, Texas. Paper number OTC 1204; 1970. p. 577–94.
[3] Robertson PK, Davies MP, Campanella RG. Design of laterally loaded driven piles using the flat dilatometer. ASTM Geotech Test J 1989;12(1):30–8.
[4] Brown DA, Shie CF. Modification of p–y curves to account for group effects on laterally loaded piles. Geotechnical engineering congress, ASCE geotechnical special publication no. 27, 1991. p. 479–90.
[5] Reese LC, Wang ST. GROUP4.0 for Windows: analysis of a group of piles subjected to axial and lateral loadings. Austin, Texas: Ensoft Inc; 1996.
[6] Mostafa YE, EL Naggar MH. Dynamic analysis of laterally loaded pile groups in sand and clay. Can Geotech J 2002;39:1358–83.
[7] Novak M. Dynamic stiffness and damping of piles. Can Geotech J 1974;11:574–98.
[8] O'Neill MW, Gazioglu SL. An evaluation of p–y relationships in clays: a report to the American Petroleum Institute. PRAC 82-41-2. Houston, Texas: The University of Houston-University Park; 1984 April.
[9] Murchison JM, O'Neill MW. Evaluation of p–y relationships in cohesionless soils. In: Proceedings of the symposium of analysis and design of pile foundations. San Fransisco: ASCE; 1984. p. 174–91.
[10] American Petroleum Institute. Recommended practice for planning, designing and constructing fixed offshore platforms. Report no.: API-RP2A. 17th ed. Washington, DC: American Petroleum Institute; 1987.
[11] Wu G. Dynamic soil-structure interaction: pile foundations and retaining structures [Dissertation] Department of Civil Engineering. Vancouver BC Canada: The University of British Columbia; 1994.
[12] Wu G, Finn WDL. Dynamic elastic analysis of pile foundations using finite element method in the frequency domain. Can Geotech J 1997;34:34–43.
[13] Wu G, Finn WDL. Dynamic nonlinear analysis of pile foundations using finite element method in the time domain. Can Geotech J 1997;34:44–52.
[14] Finn WDL, Fujita N. Piles in liquefiable soils: seismic analysis and design issues. Int J Soil Dyn Earthq Eng 2002;22:731–42.
[15] Finn WDL. Characterizing pile foundations for evaluation of performance based seismic design of critical lifeline structures. In: Proceedings of the 13th world conference on earthquake engineering. Vancouver, Canada; 2004. Paper no. 5002.
[16] Finn WDL. A study of piles during earthquakes: issues of design and analysis. Bul Earthq Eng 2005;3:141–234.
[17] Wu G, Fitzell T, Lister D. Impacts of deep soft soils and lightweight fill approach embankments on the seismic design of the Hwy. 15 North Serpentine River Bridges, Surrey, B.C. In: Proceedings of the 59th Canadian geotechnical conference. Vancouver; 2006. p. 596–601.
[18] Maiorano RMS, Aversa S, Wu G. Effects of soil non-linearity on bending moments in piles due to seismic kinematic interaction. In: Proceedings of the 4th international conference on earthquake geotechnical engineering. Thessaloniki, Greece; 2007. Paper no. 1574.
[19] Wu G. VERSAT-P3D: A computer program for dynamic 3-dimensional finite element analysis of single piles and pile groups. Wutec Geotechnical International, Vancouver, Canada. Available 〈http://www.wutecgeo.com/versat-p3d.aspx〉; 2006 [accessed 09.09.14].
[20] Finn, WDL, Wu, G. Dynamic analyses of an earthfill dam on over-consolidated silt with cyclic strain softening. In: Proceedings of the seventh international conference on case histories in geotechnical engineering, Keynote Lecture. Chicago, US; 29 April–4 May 2013.
[21] Finn WDL, Dowling J. Modelling the effects of pile diameter. Can Geotech J 2015 In press.
[22] Kaynia AM, Kausel E. Dynamic stiffnesses and seismic response of pile groups. Report R 82-03Cambridge: Department of Civil Engineering, Massachusetts Institute of Technology; 1982.
[23] Wu G, Finn WDL. Seismic lateral pressures for design of rigid walls. Can Geotech J 1999;36:509–22.
[24] Joyner WB, Chen AFT. Calculation of non-linear ground response in earthquakes. Bull Seismol Soc Am 1975;65(5):1315–36.

[25] Seed HB, Wong RT, Idriss IM, Tokimatsu K. Moduli and damping factors for dynamic analyses of cohesionless soils. ASCE J Geotech Eng 1986;112 (11):1016–32.
[26] Vucetic M, Dobry R. Effect of soil plasticity on cyclic response. ASCE J Geotech Eng 1991;111(1):89–107.
[27] Novak M, El Sharnouby B. Stiffness constants of single piles. J Geotech Eng 1983;109(7):961–74.
[28] Reese LC, Wang ST. GROUP 4.0 for Windows, analysis of a group of piles subjected to axial and lateral loading. Austin, Texas: Ensoft, Inc; 1996.
[29] Fayyazi MS, Taiebat M, Finn WDL. Group reduction factors for analysis of laterally loaded pile groups. Can Geotech J 2014;51(7):758–69.